

2017 Chinese Control Conference

Proceedings of the 36th CCC

第三十六届中国控制会议论文集



Technical Committee on Control Theory

中 文

Preface

Organizer

Plenary Speakers

Guan Z. Z. Award

Poster Award

Contents

Full Text Search

Author Index

Organizing Institutions

Technical Committee on Control Theory, Chinese Association of Automation
Systems Engineering Society of China
Dalian University of Technology

Technically Co-Sponsored by

Academy of Mathematics and Systems Science, CAS
China Society for Industrial and Applied Mathematics
Liaoning Association of Automation
Shenyang University of Chemical Technology
Liaoning University of Science & Technology
Asian Control Association (ACA)
IEEE Control Systems Society (CSS)
Institute of Control, Robotics and Systems (ICROS), Korea
The Society of Instr. and Contr. Engineers (SICE), Japan



IEEE Catalog Number: CFP1740A-USB

ISBN: 978-988-15639-3-4

ISBN 978-988156393-4



9 789881 563934

July 26-28, 2017, Dalian, China

On the Algorithm of Analyzing the Features of Magnetic Flux Leakage Signal for Pipeline Defect Based on PCA	SUN Yun, LIU Jinhai, ZHANG Huaguang	5434
Error Correction for PLC Systems Based on OFDM	ZHANG Hongyang, ZHANG Aimin	5439
Method of Navigation Resource Management Based on Efficiency Function	MU Honglei, CHENG Yongmei, GOU Bin, LIU Jianxin, LI Song	5444
Motion Control of a Four-Wheel-Independent-Drive Electric Vehicle by Motor Imagery EEG Based BCI System	ZHUANG Jiayu, YIN Guodong	5449
An Image Denoising Method Based on Nonsubsampled Contourlet Transform with SQP Optimization	YANG Chen, YU Yaozhong, LI Qingdong, DONG Xiwang, REN Zhang	5455
RGB Color Decomposition and Image Feature Extraction of Flame Image in Rear of Sintering Machine	CHEN Wu, WANG Fubin, CHEN Xianzhong, HOU Qingwen, CHEN Zhikun, ZHANG Meng, YANG Haolong	5460
Multi-focus Image Fusion Based on Multi-scale Focus Measures and Generalized Random Walk	MA Jinlei, ZHOU Zhiqiang, WANG Bo, DONG Mingjie	5464
The Variational Bayesian-Variable Structure Filter for Uncertain System with Model Imprecision and Unknown Measurement Noise	LIN Xiaogong, JIAO Yuzhao, LI Heng, KUN Liang	5469
Trajectory Tracking for Hypersonic Glide Vehicles Based on Improved Sine-AIMM	FENG Shan, TAN Qingke, LI Qingdong, REN Zhang	5475
A NEW BAYESIAN PARAMETRIC GLRT FOR MULTICHANNEL ADAPTIVE SIGNAL DETECTION	XU Qi, WANG Shenhang, LIN Ruishi, YANG Mingjun, YANG Lukun	5481
Distributed Fusion Estimation for Multi-sensor Non-uniform Sampling Systems with Correlated Noises and Packet Dropouts	LIN Honglei, SUN Shuli	5485
System Architecture Design of PCIe Root Complex Based on SOPC	LIU Yufeng, XU Degang, CAI Haiming, YANG Chunhua	5490
Design of Multiple Classifier Systems Based on Evidential Neural Network	HE Hongshun, HAN Deqiang, YANG Yi	5496
A Consensus-based Filtering Algorithm with State Constraints	MA Yajing, GUO Song, LIN Shuyi, CAI Yunze	5502
一类抗目标丢失的接力跟踪方法研究		
A Kind of Study on Relay Tracking Method for Anti-loss of Target	WANG Jing, HOU Kaiyu, HU Shan, CAI Yunze	5507
H^∞ finite-horizon filtering for discrete piecewise linear systems with infinite distributed delays and quantization effect	LI Jiajia, WEI Guoliang, ZHAO Di, WANG Jianhua	5512
An Improved Evidence Combination Approach Based on Credibility of Evidence	YU Yaozhong, YANG Chen, JIANG Hong, LI Qingdong, XIANG Jie	5518
Kalman滤波算法在激光三角法测量中的应用		
Application of Kalman Filtering Algorithm in Laser Triangulation Measurement	WEN Xiao-Qin, JUNYUAN Liang	5523
A Fast Proximal Splitting Algorithm for Constrained TGV-regularized Image Restoration	HE Chuan, LIU Lianxiong, ZHU Xiaofei, QI Naixin, HU Chang-Hua	5528
Micro Aerial Vehicle Indoor Localization Using Prior Map and Spare Sonars	XIE Qichao, YANG Lingyu, YANG Xiaoke	5534
Distributed Kalman Filtering Based on Optimal Weighting Matrix	QIU Yi, SONG Enbin, ZHU Yunmin	5539

Micro Aerial Vehicle Indoor Localization using Prior Map and Spare Sonars

Qichao Xie, Lingyu Yang, Xiaoke Yang

School of Automation Science and Electrical Engineering,

Beihang University (Beijing University of Aeronautics and Astronautics), Beijing 100191, P.R. China

E-mail: xieqichao@buaa.edu.cn; yanglingyu@buaa.edu.cn; xiaoke@hotmail.com

Abstract: Micro Aerial Vehicles(MAVs) have been seen rapid progress in the indoor entertaining, security monitoring, as well as search and rescue activities. Localization capability is one of the basis of MAVs autonomous movement and path planning. This paper proposes a novel indoor localization algorithm using a prior map for the mini MAVs with a sparse sonar array. Four mutually perpendicular installed ultrasonic sensors provide distances of each directions. An improved multiple rays model is constructed to approximate the detection range of the ultrasonic sensor. Then a maximum a posteriori (MAP) estimation of the MAV's location is accomplished using a Gaussian distribution prior and a Gaussian likelihood function. The proposed algorithm is valid on a test platform and the results indicate good localization performance and robustness against compass measurement noise.

Key Words: Indoor localization, MAV, ultrasonic sensor model, maximum a posterior estimation

1 Introduction

Indoor MAVs have wide industry applications and have been seen rapid progress in recent years^{[1][2]}. In the narrow indoor environment with obstacles, mini MAV can take full advantages of its agile characteristics to avoid the obstacles, perform rescue and mapping tasks^[2], etc.

One of the keys that MAVs can move independently and complete their missions is the autonomous localization ability. GPS is commonly used for outdoor localization, while indoor environment is lack of GPS signals. Thus localization approaches based on GPS cannot be used in indoor environment. At present, indoor localization can utilize sensors like inertial measurement unit (IMU)^[3], ranging sensors^[4], cameras^[5], Wi-Fi^[6] and ZigBee^[7], etc.

For a mini indoor MAV, constraints of the MAV size, load capacity and battery power should be considered. Laser rangefinders have high accuracy, but are not suitable for MAV because of the large size and power consumption. Cameras, especially small monocular ones, can meet the size requirements and get much more information than ultrasonic and laser rangefinders. However, the computational cost for image processing and storage is a challenge to the MAV. Ultrasonic rangefinders are smaller and lighter than laser rangefinders and cameras, and also has a lower price. So it is consistent with the requirements of the MAV in size and load capacity. But there are some shortcomings of ultrasonic sensor that cannot be ignored, such as the measurement range limitation, multi-lobe distribution and the poor angle resolution.

Based on the above analyses, an indoor localization approach combining an IMU and an array of ultrasonic rangefinders under a prior map is adopted in this paper.

Research of ultrasonic indoor localization has been carried out for many years. In [8], the ultrasonic characteristics and the distribution of the lobes were

analyzed in detail. The boundary and angle of ultrasonic lobes were measured by moving an obstacle and reading the sensor values. Finally, an accurate mathematical model was established.

A cone model with a probability distribution is also used for describing the ultrasonic characteristics. The sensor heading is set as the origin and the ultrasonic multi-lobe distribution is assumed to be a cone. When the obstacle is close to the ultrasonic central axis, the probability of the measured value is high, when away from the central axis, the probability of the measured value is low. In [9], "occupancy probabilities" was used to describe the result of obstacle detection. When the ultrasonic sensor received the measured signal, the product of a distance probability and an angle probability was taken as the probability of the obstacle location. In [10], based on the cone model, a Triangulation Based Fusion (TBF) algorithm was proposed to extract features from the measured values for building environmental map and achieving the localization estimation. In [11], 16 ultrasonic sensors were used to extract landmarks and match the map for estimating the location. The result showed an accuracy of 5-15cm. TBF algorithm is also investigated in [12] and [13]. In [12], a robot pose tracking algorithm based on the TBF was experimented in a large-scale indoor environment. In [13], a TBF algorithm with added line feature extraction was used for extracting intersections based on 12 ultrasonic sensors surrounded the mobile robot. In [14], firstly, the data of eight frontal ultrasonic sensors was obtained based on evidence grids, then fast Fourier transform was used to filter out the noise for the obstacle contours and finally the short feature vectors were obtained based on principal components analysis (PCA). In [15], a novel data fusion localization algorithm was proposed and applied to the framework which is based on the extended Kalman filter (EKF). In [16], the results of the ultrasonic occupancy grids based on Bayesian, Dempster-Shafer evidence theory and fuzzy set theory were analyzed and compared. In [17], the ultrasonic data acquisition was divided into two steps: Firstly, combine

travelling and stopping. Secondly, rotate the angle. The mathematical model was made up of the directional probability and the measured value estimation. The average and least squares method were used to fit, then the local map and global map were established. In [18], TBF, Hough transform (HT) and sonar salient (SS) feature algorithms were combined to extract the features.

Compared with the above literatures, the main contributions of this paper are concentrated as the following two aspects:

Firstly, apart from [8], the ultrasonic models in the other literatures are improved based on the cone model. The cone model is poor in distinguishing the angle of obstacles. The conical approximation to the real distribution of ultrasonic lobes can also exhibit large errors. In this paper, the measurement boundary of the ultrasonic sensor is measured, and a "polygon" model is established precisely, which reflects the actual ranging boundary of the used ultrasonic sensor.

Secondly, for most of MAVs and mobile robots which use ultrasonic sensors, some use a single ultrasonic sensor, and some use multiple ultrasonic sensors aligned on a circle with equal spaces. A single ultrasonic sensor provides limited information while too many ultrasonic sensors are not suitable for MAV due to its load capacity and power consumption. In this paper, the MAV is equipped with four ultrasonic sensors aligned at right angles for a balance between information acquisition and the limitation of the MAV platform.

The framework of this paper is organized as follows: the ultrasonic mathematical model is established in the second section; indoor localization is discussed in detail in the third section; in the fourth section, an experiment is carried out in an indoor environment with no obstacles. Robustness is also tested under compass measurement noise.

2 Ultrasonic Measurement Model

The ultrasonic sensor used in this paper is a single transducer ultrasonic rangefinder named SRF01^[19]. The net weight of SRF01 is 3g and its diameter is about 1.6cm. The official datasheet indicates that the measurement distance is 18cm to 600cm in standard mode. The minimum measurement distance in advanced mode can be reduced to 0cm. Furthermore, the minimum measurement time interval is least 70ms. Summarizing the above features of SRF01, it's suitable for the MAV platform.

Fig.1 shows the original detection range of SRF01. It is obtained by placing and measuring an obstacle in the positions of a predefined grid points in front of the ultrasonic sensor.

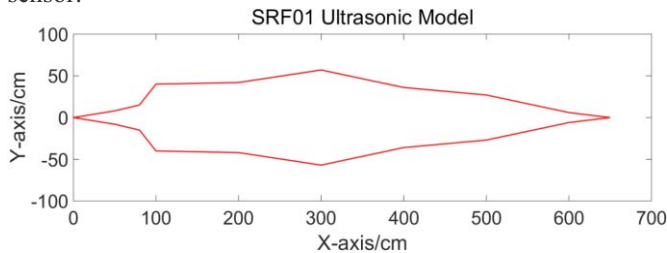


Fig.1 SRF01 contour model (without cloth tube)

Fig.1 shows that SRF01 measurement range is a polygon. The left and right boundaries exceed 50 cm at 300 cm distance, showing its poor angle resolution for localization.

To improve the angle resolution of the SRF01 model, the side lobes are suppressed by a 0.5cm cloth tube. The axial cross section of the SRF01 measurement range with cloth tubes is shown in Fig.2.

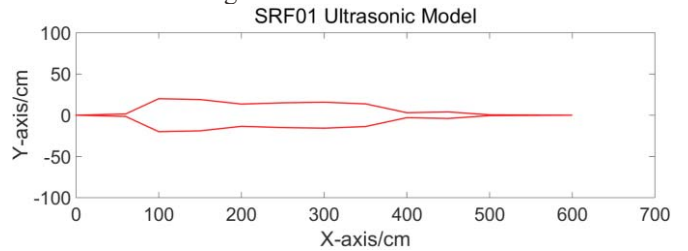


Fig.2 SRF01 contour model (with cloth tube)

Fig.2 shows that the detection boundary is significantly concentrated and the maximum width of the lobe is less than 20cm, which improves the angle resolution.

Based on the ultrasonic contour model, a SRF01 multiple rays model in Fig.3 is obtained by connecting the sensor heading to the points of the contour model detection boundary.

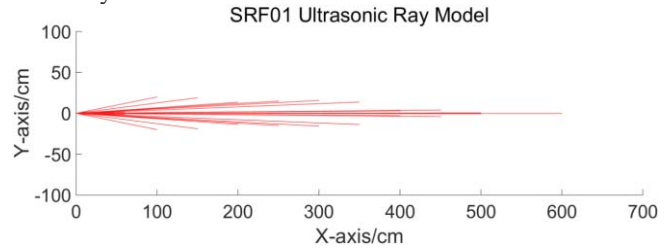


Fig.3 SRF01 multiple rays model (with cloth tube)

The multiple rays model will be applied to the ultrasonic estimation algorithm in the third section.

The ultrasonic multiple rays model is expressed as:

$$\begin{cases} \mathbf{S} = \{\mathbf{s}_0, \mathbf{s}_1, \mathbf{s}_2, \dots, \mathbf{s}_l\} \\ \mathbf{s}_0 = [x_s, y_s]^T \\ \mathbf{s}_j = [x_s + d_j \cos(\psi + \gamma_j), y_s + d_j \sin(\psi + \gamma_j)]^T \quad (j = 1 \dots l) \end{cases}, \quad (1)$$

where ψ is the angle of ultrasonic central axis, d_j is the length of the j^{th} ray, γ_j is the angle of the j^{th} ray relative to the central axis. The estimated measurement of the ultrasonic multiple rays model is

$$u = \min(\|\mathbf{q}_1 - \mathbf{s}_0\|_2, \|\mathbf{q}_2 - \mathbf{s}_0\|_2, \dots, \|\mathbf{q}_l - \mathbf{s}_0\|_2), \quad (2)$$

where $\mathbf{q}_j = [x_j, y_j]^T$ is the intersection of the external environment and the j^{th} ray.

Compared to the contour model, multiple rays model needs less computing resource in the localization estimation. However, the multiple rays model also brings localization errors. The model resolution and the maximum measurement error are analyzed in the following part.

When the obstacle is between two adjacent rays and the radius is less than a certain value, the obstacle will not be detected by the ray model. Let the radius of the obstacle is r when the edge of the obstacle is tangent to the two adjacent rays, we can get the resolution

$$r = d_o \cdot \sin \frac{\Delta\gamma}{2}, \quad (3)$$

where d_o is the distance from the center of the obstacle to the ultrasonic sensor and $\Delta\gamma = \gamma_{j+1} - \gamma_j$.

When the obstacle is just on the contour, we can get the maximum measurement error

$$\Delta d = d_{j+1} - d_j, \quad (4)$$

where d_j is the length of the j^{th} ray.

When the obstacle is inside the ultrasonic contour, the multiple rays model error is related to the angle of the wall and the ultrasonic central axis.

Let the angle between the wall and the ultrasonic central axis is φ , the maximum error is

$$u_{\text{error}} = u(1 - \sin(\varphi + \gamma_j)), \quad (5)$$

where j represents the j^{th} ray that minimizes Eq.(2).

3 Indoor Localization Algorithm

Based on the multiple rays model, a maximum a-posteriori (MAP) algorithm is used to estimate the MAV location.

MAP is based on the observed data x so that the posterior probability density function of $f(\theta|x)$ reaches the maximum value.

After taking the logarithm according to the Bayesian equation, we can get

$$\hat{\theta}_{\text{MAP}}(x) = \arg \min_{\theta} [\log f_1(\theta) + \log f_2(x|\theta)]. \quad (6)$$

Specific to the localization algorithm, the detection interval of ultrasonic sensors is 0.1s and the moving distance of MAV is short in 0.1s. Based on the above assumption, the present location is regarded as a Gaussian distribution centered on the previous location, i.e., $f_1(\theta)$ represents the Gaussian distribution of the estimated location. Similarly, the actual readings are regarded as Gaussian distributions centered on the theoretical readings, i.e., $f_2(x|\theta)$ represents the Gaussian distribution of the actual ultrasonic sensor readings.

So $f_1(\theta)$ and $f_2(x|\theta)$ can be written as follows

$$f_1(\theta) = \frac{1}{\sqrt{(2\pi)^2 |\Sigma_1|^{1/2}}} \cdot \exp \left\{ -\frac{1}{2} (\mathbf{v}(k) - \hat{\mathbf{v}}(k-1))^T \Sigma_1^{-1} (\mathbf{v}(k) - \hat{\mathbf{v}}(k-1)) \right\} \quad (7)$$

$$f_2(x|\theta) = \frac{1}{\sqrt{(2\pi)^4 |\Sigma_2|^{1/2}}} \cdot \exp \left\{ -\frac{1}{2} (\mathbf{u}_m(k) - \mathbf{u}(k))^T \Sigma_2^{-1} (\mathbf{u}_m(k) - \mathbf{u}(k)) \right\} \quad (8)$$

In Eq.(7) and Eq.(8), the k is the sampling time, $\mathbf{M} \in \mathbf{R}^{2 \times N}$ represents the environment and consists of N environment corner locations in counterclockwise direction from the origin. $\mathbf{v}(k) \in \mathbf{R}^2$ is the location of MAV and $\hat{\mathbf{v}}(k) \in \mathbf{R}^2$ is the estimated location. $\mathbf{u}_m(k) \in \mathbf{R}^4$ is the measurement vector of the four ultrasonic sensors and

$\mathbf{u}(k) \in \mathbf{R}^4$ is the estimation of $\mathbf{u}_m(k)$. Σ_1 and Σ_2 are covariance matrices and we assume that each element of $\mathbf{u}(k)$ and $\mathbf{v}(k)$ is independent of each other and has the same variance, i.e. Σ_1 and Σ_2 are unit diagonal matrices.

Substituting Eq. (7) and Eq. (8) into Eq. (6) yields the optimization function

$$\hat{\mathbf{v}}(k) = \arg \min_{\mathbf{v}(k)} \left[\begin{array}{l} \lambda_1 \cdot \|\mathbf{v}(k) - \hat{\mathbf{v}}(k-1)\|_2^2 \\ + \lambda_2 \cdot \|\mathbf{u}_m(k) - \mathbf{u}(k)\|_2^2 \\ + \log(|\lambda_1| \cdot \lambda_2^2 / \pi^3) \end{array} \right], \quad (9)$$

where $\lambda_1 = -\frac{1}{2 \cdot \sqrt{|\Sigma_1|}}$ and $\lambda_2 = -\frac{1}{2 \cdot \sqrt{|\Sigma_2|}}$.

Since the constant term in Eq.(9) does not affect the optimization result, we can rewrite optimization function as

$$\hat{\mathbf{v}}(k) = \arg \min_{\mathbf{v}(k)} \left[\begin{array}{l} \lambda_1 \cdot \|\mathbf{v}(k) - \hat{\mathbf{v}}(k-1)\|_2^2 \\ + \lambda_2 \cdot \|\mathbf{u}_m(k) - \mathbf{u}(k)\|_2^2 \end{array} \right]. \quad (10)$$

The constraint of Eq.(10) is that $\mathbf{v}(k)$ must be within the map defined by \mathbf{M} .

$\mathbf{u}(k)$ can be written as

$$\mathbf{u}(k) = g(\mathbf{v}(k), \psi(k), \mathbf{M}, \mathbf{S}), \quad (11)$$

where $\psi(k)$ is the MAV yaw angle obtained from the magnetic compass.

We can obtain $\mathbf{u}(k)$ from the following algorithm.

Algorithm 1 g function algorithm

Inputs: $\mathbf{v}(k), \psi(k), \mathbf{M}, \mathbf{S}$

Process: $\mathbf{u}(k) = g(\mathbf{v}(k), \psi(k), \mathbf{M}, \mathbf{S})$

1: **if** $\mathbf{v}(k)$ is within \mathbf{M} **then**

2: Initialize the intersection of \mathbf{S} and \mathbf{M}

3: Get the rotation matrix $\psi(k)$ of four ultrasonic sensors

$$\psi(k) \rightarrow [\psi_1(k) \quad \psi_2(k) \quad \psi_3(k) \quad \psi_4(k)]^T$$

4: **for** $i = 1 \rightarrow 4$ **do**

5: **for** $j = 1 \rightarrow l$ **do**

6: Based on $\mathbf{v}(k)$ and $\psi(k)$, the intersection of \mathbf{M} and

$$\text{the } j^{\text{th}} \text{ ray: } \mathbf{q}_j(k) \in \mathbf{R}^{2 \times l}$$

7: **end**

8: $\min(\|\mathbf{q}_1(k) - \mathbf{s}_0\|_2, \|\mathbf{q}_2(k) - \mathbf{s}_0\|_2, \dots, \|\mathbf{q}_l(k) - \mathbf{s}_0\|_2) \rightarrow \mathbf{u}(k)$

9: **end**

Output: $\mathbf{u}(k)$

The flow chart of the proposed indoor localization algorithm is shown in Fig.4.

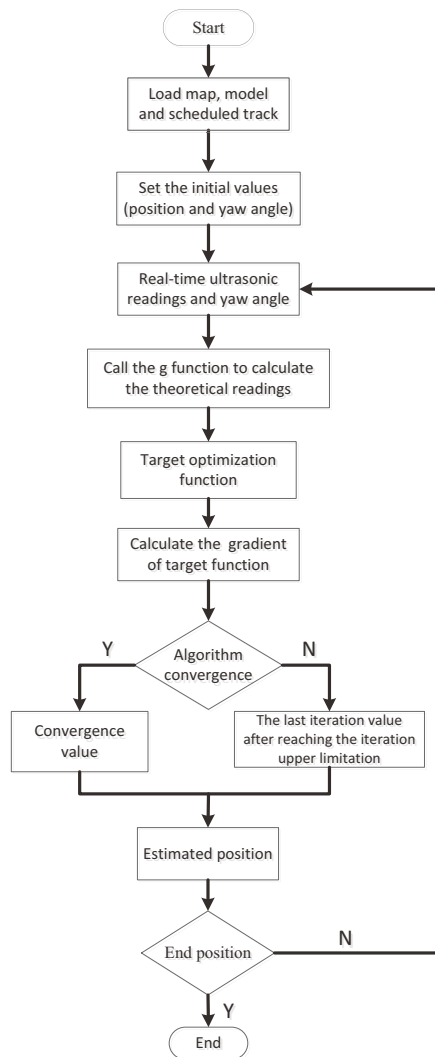


Fig.4 The flow chart of indoor localization algorithm

4 The Experimental Results

An experimental platform is made before installing the ultrasonic sensors on MAV. The four mutually perpendicular ultrasonic sensors are numbered from 1 to 4 in clockwise, which is shown in Fig.5 and Fig.6.

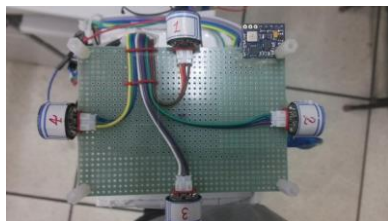


Fig.5 The mobile experimental platform (without cloth tube)

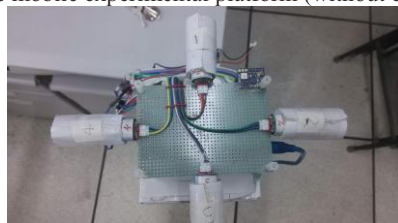


Fig.6 The mobile experimental platform (with cloth tube)

An indoor space without obstacles is selected as the experimental area, and the trajectory and direction of the MAV are set as shown in Fig.7.

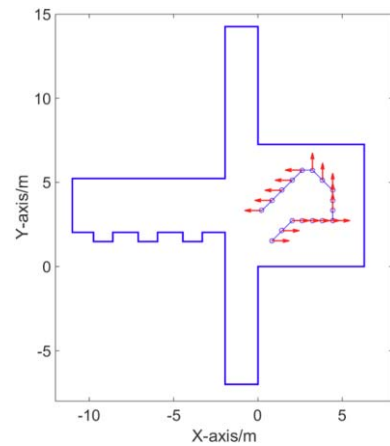


Fig.7 Experimental environment and MAV trajectory

The blue border represents walls in the experimental environment, the blue circles represent the sampling locations of the ultrasonic sensors, and the red arrows represent the directions of the MAV yaw at the sampling locations.

The initial location of the MAV is (0.8m, 1.5m), the yaw angle $\psi(0)$ is 0. λ_1 is set as 0.2, λ_2 is set as 0.8 and the maximum number of iterations is set as 10. The localization algorithm is applied to the MAV platform for real-time testing and the estimated locations are shown in Fig.8.

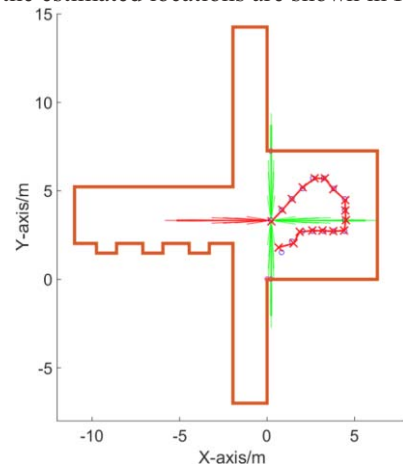


Fig.8 The result of MAV real-time localization estimation

Fig.8 shows the estimated location calculated by the proposed ultrasonic multiple rays model and the localization algorithm.

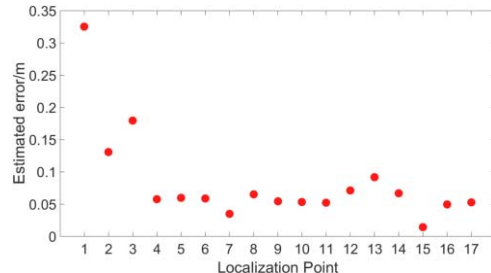


Fig.9 Localization estimation error (without Gaussian noise)

Fig.9 shows the result of the location errors without Gaussian noise. We can see that the error of the initial point is the largest, and the errors of the other points are mostly within 0.1m. The average error of the estimated distance is 0.0835m, which indicates that the localization algorithm is effective.

In actual measurement, there is an error between the value of magnetic compass and the real MAV yaw angle. To verify

the robustness of the localization algorithm, a certain intensity of Gaussian noise is added to $\psi(k)$.

When adding Gaussian noise with mean 0 and standard deviation of 5° , we get a set of location errors as follows:

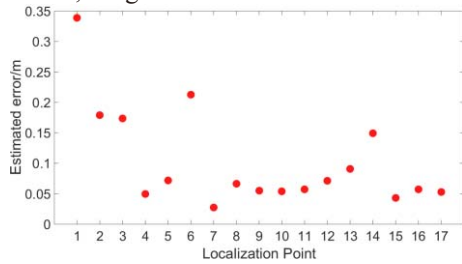


Fig.10 Localization estimation error (with Gaussian noise)

The result shows that the localization errors don't change significantly with Gaussian noise. The average error of all measurement points is 0.1030m, which reflects the good robustness of the localization algorithm.

5 Conclusion

In this paper, a multiple rays model of the ultrasonic sensor SRF01 is established and the angular resolution of the ultrasonic sensor is improved by a cloth tube. Based on the improved ultrasonic model and a prior map of the environment, an indoor MAV localization algorithm is designed. Under the condition of a prior map, the array of four mutually perpendicular ultrasonic sensors and the yaw angle data, MAV localization algorithm is carried out. The results verified the accuracy of localization. In addition, Gaussian noise is added to the yaw angle and the result shows that the localization algorithm has good robustness. The next step is to integrate the proposed algorithm with other type of sensors such as small monocular camera.

References

- [1] Scaramuzza, Davide, et al. "Vision-Controlled Micro Flying Robots: From System Design to Autonomous Navigation and Mapping in GPS-Denied Environments." *IEEE Robotics & Automation Magazine* 21.3(2014):26-40.
- [2] Ahn, Young Min, D. J. Block, and R. S. Sreenivas. "Autonomous Navigation and Localization of a Quadrotor in an Indoor Environment." *Journal of Aerospace Information Systems* 12.12(2015):1-11.
- [3] Hoflinger, F, R. Zhang, and L. M. Reindl. "Indoor-localization system using a Micro-Inertial Measurement Unit (IMU)." *European Frequency and Time Forum IEEE*, 2012:443-447.
- [4] Cho, Shung Han, and S. Hong. "Map based indoor robot navigation and localization using laser range finder." *International Conference on Control Automation Robotics & Vision IEEE*, 2010:1559-1564.
- [5] Yuen, D. C. K, and B. A. Macdonald. "Vision-based localization algorithm based on landmark matching, triangulation, reconstruction, and comparison." *Robotics IEEE Transactions on* 21.2(2005):217-226.
- [6] Fan, Heng, and Z. Chen. "WiFi based indoor localization with multiple kernel learning." *IEEE International Conference on Communication Software and Networks IEEE*, 2016:474-477.
- [7] Niu, Jianwei, et al. "ZIL: An Energy-Efficient Indoor Localization System Using ZigBee Radio to Detect WiFi Fingerprints." *IEEE Journal on Selected Areas in Communications* 33.7(2015):1-1.
- [8] Hanzel, Jaroslav, et al. *Identification Based Model of Ultrasonic Sensor. Research and Education in Robotics - EUROBOT 2011*. Springer Berlin Heidelberg, 2011:144-157.
- [9] Elfes, Alberto. "Sonar-based real-world mapping and navigation." *IEEE Journal on Robotics and Automation* 3.3(1990):249-265.
- [10] Wijk, O, P. Jensfelt, and H. I. Christensen. "Triangulation based fusion of ultrasonic sensor data." *IEEE International Conference on Robotics and Automation, 1998. Proceedings IEEE*, 1998:3419-3424 vol.4.
- [11] Wijk, Olle, and H. Christensen. "Extraction of Natural Landmarks and Localization using Sonars." *Proc.~of the International Symposium on Intelligent Robotic Systems* 1998:231--240.
- [12] Wijk, O., and H. I. Christensen. "Triangulation-based fusion of sonar data with application in robot pose tracking." *IEEE Transactions on Robotics & Automation* 16.6(2000):740-752.
- [13] Weiqin, Zheng. "Sonar Features Extraction Algorithm for a Mobile Robot." *Third International Symposium on Intelligent Information Technology Application IEEE Computer Society*, 2009:689-692.
- [14] Poncela, A, et al. "A New Sonar-based Landmark for Localization in Indoor Environments." *Soft Computing* 11.3(2007):281-285.
- [15] Park, Joong Tae, et al. "Sonar Sensor-Based Efficient Exploration Method Using Sonar Salient Features and Several Gains." *Journal of Intelligent & Robotic Systems* 63.3(2011):465-480.
- [16] Ribo, Miguel, and A. Pinz. "A comparison of three uncertainty calculi for building sonar-based occupancy grids." *Robotics & Autonomous Systems* 35.3-4(2001):201-209.
- [17] Noykov, Sv, and C. Roumenin. "Occupancy grids building by sonar and mobile robot." *Robotics & Autonomous Systems* 55.2(2007):162-175.
- [18] Ismail, Hesham, and B. Balachandran. "Algorithm Fusion for Feature Extraction and Map Construction from SONAR Data." *IEEE Sensors Journal* 15.11(2015):6460-6471.
- [19] SRF01 Ultrasonic range finder Technical Documentation [EB/OL].<https://www.robot-electronics.co.uk/htm/srf01tech.htm>,2017-05-09.